Available online at www.sciencedirect.com
SCIENCE DIRECT®
Estuarine, Coastal and Shelf Science 61 (2004) 379–392
ESTUARINE COASTAL AND SHELF SCIENCE
www.elsevier.com/locate/ECSS

Detection of estuarine and tidal river hydromorphology using hyper-spectral and LiDAR data: Forth estuary, Scotland

David Gilvear*, Andrew Tyler, Corine Davids

School of Biological and Environmental Sciences, University of Stirling, FK9 4LA, Scotland

Received 26 January 2004; accepted 3 June 2004

Abstract

High spatial resolution hyper-spectral imagery (CASI) and light detection and ranging (LiDAR) imagery acquired for the tidal River Carron and Forth estuary, Scotland, were used in conjunction with field surveys to assess the feasibility of monitoring hydromorphology and human alterations with satellite and airborne remote sensing data. The study was undertaken in the context of the European Union Water Framework Directive (WFD) that requires member states to monitor hydromorphological elements as a component of the ecological status of rivers, estuaries and shorelines. Visual assessment and automated classifications of the imagery were compared with field survey data for an estuarine reach comprising saline waters, mudflats, a tidal reach of a tributary river and an urban/industrialised shoreline.

The morphology of the estuary and inflowing tidal waters together with most artificial features of interest could be clearly seen in the CASI imagery at 1 m spatial resolution. Supervised classification of the imagery produced an overall accuracy value of 72%. Downgrading the imagery to simulate the spatial resolution of 4 m IKONOS satellite data surprisingly improved the accuracy to 74%. Simulation of 10 m SPOT imagery resulted in an image where many artificial features of interest such as roads, pipelines and jetties were rendered invisible. Adding LiDAR data as an additional data set aided manual and automated identification of features and visualisation of the hydromorphology of the rivers and estuaries in the study area. Shadows cast from tall objects were a feature of the winter imagery and reduced automated classification accuracy.

Overall, the study demonstrates that high spatial resolution remotely sensed digital imagery has the potential to be a useful tool for panoptic mapping of the geomorphology and human impact on tidal rivers and estuaries. In the context of the WFD, remote sensing provides a potential way forward for monitoring the physical status of rivers and estuaries at the national scale. The possibilities and constraints, in light of the findings of this study, are discussed.

Keywords: airborne remote sensing; geomorphology; estuaries; satellites; rivers; river and coastal engineering

1. Introduction

Surveying the morphology of river channels, estuaries and coastal shorelines and the level of physical habitat degradation due to human activity has traditionally been conducted in the field. In some cases, hard-copy aerial photography has been used alongside field surveys to facilitate more accurate mapping. The drawback of such field surveys is that they are local in extent, time consuming, relatively costly and until the advent of cheap relatively accurate global positioning systems the data were not geo-referenced. Remotely sensed digital imagery, however, provides a potential means of gaining synoptic coverage of estuarine and river systems and monitoring change, that is potentially less costly on a long-term basis (Muller et al., 1993; Yates et al., 1993; Donoghue et al., 1994; Milton et al., 1995; McManus et al., 1999; Gilvear et al., 1999, in press; Leuven et al., 2002; Rainey et al., 2003). Many remote sensing sensors

* Corresponding author.
E-mail address: d.j.gilvear@stir.ac.uk (D. Gilvear).

0272-7714/$ - see front matter
doi:10.1016/j.ecss.2004.06.007

also have the potential to interrogate the Earth's surface in specific wavelengths, to assess reflectance in wavelengths beyond the visible spectrum and in some cases to measure the elevation of the terrain beneath the sensor. This may therefore allow detection of features not visible to the naked eye. Sensors are usually either mounted on aircraft or satellite platforms. Generally sensors mounted on aircraft have higher spatial and spectral capabilities but provide more restricted spatial coverage and are more demanding in terms of computer space and image processing. Traditionally satellite data have come with a spatial resolution of 10 or more metres (e.g. Landsat TM; SPOT). With a new generation of satellites, a spatial resolution of 1 m is now also possible in panchromatic format (IKONOS) while multi-spectral capability is available at 4 m (i.e. IKONOS; QUICKBIRD). Selection of the best sensor and platform for a particular application is a key remote sensing issue (Gilvear and Bryant, 2003).

In the context of using remote sensing to map estuary and river hydromorphology and artificial features, the first and primary concern is that of scale. A number of studies of estuaries and large rivers (>200 m wide) have been undertaken using satellite remote sensing and more recently during space shuttle missions. Milton et al. (1995) suggest that for small and medium size rivers (approx. 20–200 m wide), airborne remote sensing, incorporating high resolution advanced sensors and improved temporal/spatial flexibility, may be a more suitable approach for mapping and monitoring change. Estuaries with their wider expanse lend themselves to mapping, via both airborne and spaceborne sensors, and a large number of studies are therefore found (e.g. Thomson et al., 1998; Rainey et al., 2003; Yates et al., 1993).

A number of recent studies have demonstrated the utility of digital airborne imagery for mapping estuarine and channel morphology (e.g. Winterbottom and Gilvear, 1997; Westaway et al., 2000; Wright et al., 2000; van der Wal et al., 2002), suspended sediments, inter-tidal substrates (e.g. Batholdy and Folving, 1986; Hardy et al., 1994; Bryant et al., 1996; Thomson et al., 1998; Horritt et al., 2003) and geomorphic change (Bryant and Gilvear, 1999). Wright et al. (2000) showed the possibility of automated classification and mapping of hydromorphic stream units on two creeks of 16–180 m width in Montana and Wyoming using 1 m resolution 4 waveband ADAR imagery. Comparison of the unsupervised classification with field mapping gave total correctly classified pixel accuracies of 11–53%. Some of the inaccuracy was solely the result of poor image orthorectification with errors of up to 5 m. The researchers also found confusion with some physically different features such as bars and 'broken' surface water having similar spectral properties when viewed using only 4 bands. Whited et al. (2002) also using 0.7 m 4 waveband imagery mapped in-stream habitat on the Yakima River, USA. Classification accuracies for islands, exposed rocks and water surfaces were greater than 99% but identification of hydraulic habitat (riffles, eddies, slack water and pools) was less accurate (70%), including steps to remove the problems of misclassification due to shadow by manual removal. Cast shadow appears to be a common problem in such applications. Light detection and ranging (LiDAR) data have also been used to map bank morphology and riparian vegetation structure (Witte et al., 2001) together with floodplain morphology (Cobby et al., 2001; Charlton et al., 2003). Bryant and Gilvear (1999), using 2 m resolution 11 waveband airborne thematic mapper (ATM) imagery, collected either side of a large flood, also identified changes in morphology and riparian habitats via automated classification and change detection algorithms. Similarly, Atkin (pers. comm.) mapped flood tide suspended sediment dynamics and loading using multiple images of the Ribble estuary, England, collected over a rising tide. A key issue with regard to coastal environments is tidal conditions. Rainey et al. (2003) showed that to distinguish whether inter-tidal substrates were sand, silt or clay, imagery had to be acquired at low tide following a period of substantial drying. High soil moisture contents masked the difference between spectral signatures immediately following the ebb tide. These studies together demonstrate the utility of remotely sensed data to map estuaries and tidal rivers at high spatial and temporal resolution.

The study presented here was undertaken in the context of the European Union Water Framework Directive (WFD) (2000/60EC) which requires member states to monitor hydromorphological elements of rivers, lakes, estuaries and coastlines as a component of ecological status. The environmental objectives of the WFD are to prevent deterioration in ecological status and restore "good status" by 2015. Good ecological status allows only a slightly greater level of human alterations than it would at its reference level. For waters not designated as heavily modified or artificial, the reference conditions are synonymous with high ecological status. Good ecological status is based on biological, physico-chemical and hydromorphological quality elements. Hydromorphological elements are: hydrological regime, quantity and dynamics of water flows, connection to groundwater bodies, river continuity, morphological conditions, water depth and width variations, structure and substrate of the riverbed and structure of the riparian zone. Some surface waters have been substantially physical altered for activities such as navigation, water storage and flood defence and it is unfeasible for them to reach good ecological status. Such waters will be designated "Heavily Modified". The initial phase of the WFD process requires Member

States to produce a Characterisation Report for each River Basin District by the end of 2004. This includes reporting on "hydromorphological" quality elements, namely hydraulic habitat and channel morphology, and "hydromorphic alteration and their impacts". The latter includes the presence of man-made features and management activities such as channelisation and land claim, together with geomorphological consequences, such as changes in substrate type, and extent of exposed sediments and changes in wetted perimeter.

The overall aim of the study was to examine the feasibility of using hyper-spectral data from satellite and airborne sensors to detect and map at the national scale the key hydromorphic attributes of tidal rivers and estuaries necessary to comply with the WFD. As indicated above there are widespread assertions that remotely sensed data are ideally suited to panoptic mapping of rivers and estuaries but few studies have explored the reality of the process and accuracy in relation to the needs of end-users. The results presented here relate to the use of CASI and LiDAR data on a reach of the Forth estuary encompassing a tidal reach of the River Carron, Scotland. The study was undertaken alongside a trial of digital colour photography and multi-spectral imagery for mapping hydromorphology on non-tidal river systems (Gilvear et al., in press).

2. The study area

The Forth estuary is located on the eastern seaboard of Scotland and drains into the North Sea (Fig. 1). The tidal range is 5.0 m on spring tides and 2.5 m on neap tides when measured at Rosyth. The highest tides occur in February–March and in October–November (6.2 m and 6.3 m). In June–July the highest tide is about 5.7 m. Average salinity levels vary from 25 at Queensferry to 10 at Alloa (Fig. 1), but these values vary widely dependent on freshwater inflow and tidal condition. More than 50% of inter-tidal areas were reclaimed in the 20th century (McClusky, 1987). However the estuary has extensive mudflats and marshes which are partially covered at high tide. The city of Edinburgh borders the estuary's southern shoreline. To the east many industrial areas, the largest being Grangemouth oil refinery, line the shoreline. A number of bridges also cross the estuary most notably at Queensferry and Kincardine. Eight major rivers provide the freshwater input into the estuary. The combined freshwater discharges from the rivers Teith, Forth and Allan constitute on average 75% of the total freshwater flow to the estuary (Webb and Metcalfe, 1987). The next largest freshwater input is from the River Carron that drains a catchment area of 240 km^2 to the south-west of the industrial complex of Grangemouth and enters the estuary midway between the tidal limit and the North Sea.

Imagery for the whole of the Forth estuary was initially visually surveyed to assess its full potential and possible limitations when used for synoptic monitoring of hydromorphology and artificial features of numerous estuaries around Scotland. For quantitative analysis, a representative reach encompassing saline waters, mudflats, a tidal reach of an inflowing river and an urban/industrialised shoreline were selected. This covered 10 km of estuary including both northern and southern shores between the Kincardine Bridge and Grangemouth including the tidal reaches of the River Carron. The northern shore of the estuary for much of

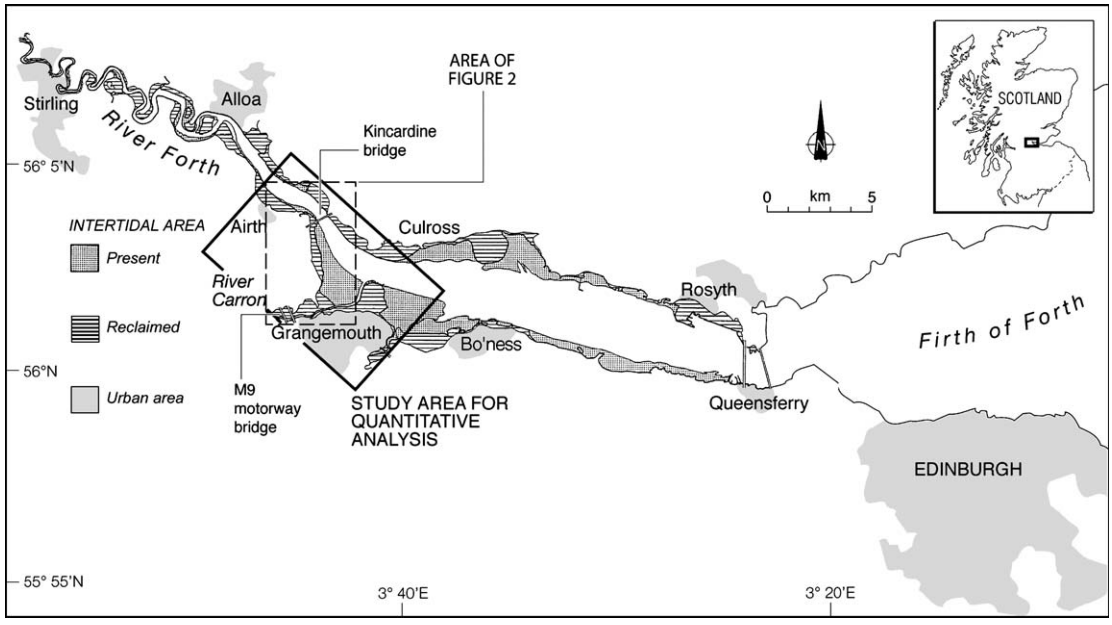

Fig. 1. The River Forth estuary showing its geography and location of the main study area.

its length in the study area is reinforced by concrete and rip-rap. Near the Kincardine Bridge, several concrete and grass-covered jetties and piers, metal pipes and outfalls also exist. A grass covered flood embankment with a width of approximately 4 m, runs along the southern shore and alongside the northern bank of the River Carron. On the southern side of the river, bank protection consists of rip-rap and wooden and concrete walls.

3. Methods

3.1. Imagery acquisition and basic processing

3.1.1. CASI

The CASI 1 m resolution imagery for the study area covers an area of approximately 60 km^2 between Airth, Kincardine and Grangemouth. The area is covered by 12 parallel SSE-NNW flight lines with a swath width of approximately 514 m. Overlap between adjacent flight lines varied from 25 to 75%. The imagery has 19 bands with wavelengths between 440 and 1000 nm (waveband ranges are detailed in Table 1) and is georectified to the British National Grid (Transverse Mercator Projection); with a root mean square error of 1.24 m. The imagery was acquired during the winter of 2001–2002 at low tide between 12:30 h and 13:30 h Greenwich Mean Time. At this time skies were cloudless and the sea conditions calm.

Despite being acquired around noon, the imagery is characterised by shadows cast from trees, buildings and bridges. This reflects the low winter sun angle and northerly latitude of the study area (56°N). In some cases this leads to the masking of the features present. For example, the shadows of industrial buildings along the southern side of the River Carron mask the southern river bank. Limb brightening effects (uneven brightness across the image) were also apparent on the image. This occurs because of variation in path radiance, caused by a variation in view angle and orientation of the flight path relative to the sun's azimuth. The limb brightening effects are minimised when the flight path is parallel to the sun's azimuth as was the case here; the imagery was acquired along flight paths that were orientated more or less parallel to the sun's azimuth, SSE-NNW. Correction for limb brightening was not possible because the imagery was geocorrected and limb brightening needs to be undertaken on the raw data. Atmospheric correction was also not undertaken. However, in this semi-empirical application the effect is likely to be minimal. The 1 m resolution CASI data were also degraded to 4 m and 10 m spatial resolution to produce 3 datasets. This was undertaken to examine the effect of pixel sizes, equivalent to the spatial resolution of QUICKBIRD and IKONOS multi-spectral satellite imagery, on feature recognition and hydromorphology detection. No other analysis was undertaken with the raw imagery being used.

Table 1
Details of waveband ranges of the 19-band CASI imagery

Band number	Waveband ranges (nm)	Spectral region
1	440–450	Blue
2	465–475	Blue
3	485–495	Blue
4	545–555	Green
5	593–603	Green
6	620–630	Red
7	660–665	Red
8	665–675	Red
9	680–685	Red
10	695–705	Red
11	705–715	NIR (Near infrared)
12	715–725	NIR
13	745–755	NIR
14	760–765	NIR
15	775–785	NIR
16	855–865	NIR
17	870–890	NIR
18	900–925	NIR
19	935–1000	NIR

3.1.2. LiDAR

The LiDAR altimetry data used in this study were collected in January 2002 by the Environment Agency UK, using an Optech ALTM1020 LiDAR system. The data were supplied for the study area in ASCII format and include a surface model, which includes all objects such as trees and buildings, a bare-earth surface model, which is the surface minus the objects, and an object layer. The point density is equivalent to about 1 measurement about every 7 m^2 with interpolation to a 2 m × 2 m grid.

3.2. Image analysis

Both unsupervised and supervised classifications were carried out on the three CASI data sets. Unsupervised classification was undertaken using the ISODATA algorithm in Erdas Imagine 8.5. The algorithm classifies the image into a pre-selected number of classes using an iterative calculation procedure to ensure maximum statistical separability on the basis of the spectral data. The image was classified into 50 classes. For the supervised classification the image was classified into 13 target classes: namely buildings, tarmac roads, railway track, metal outfalls, concrete, rock boulders (rip-rap), mudflats, saline water, freshwater, saltmarsh, grass, cereals, and woodland. Supervised classification is based on training areas that are selected as representative of desired target classes. For each target class the Erdas Imagine software calculates a statistical spectral signature based on the spectral data in the training

areas. The spectral signature is then used to extrapolate the classification across the area of interest using the maximum likelihood classifier. This approach can therefore sometimes gain higher accuracy than possible with an unsupervised classification method.

Accuracy assessment was carried out using Erdas Imagine's built-in accuracy assessment method. This method generates a pre-selected number of random points across the classified image. The software determines the class of each random point on the classified image by taking the class that forms the majority within a 3×3 pixel cell. The user identifies the correct target class for each of these points as a reference. The software compares the classes of the classified image with the reference data for each of the random points and calculates an error matrix. The error matrix shows how the classification represents actual areas in the landscape and to what classes incorrectly classified pixels were assigned. Two types of accuracy can be calculated from the error matrix: the *producer's accuracy* indicates how much of the actual landscape is correctly classified on the classified image. The *user's accuracy*, by contrast, indicates the reliability of the map by stating how much of the classified image corresponds to the same class in the actual landscape.

3.3. Field survey

Field observations involved a walk-over survey determining all the major morphological and habitat features together with man-made features present in the reach and marking their presence on a copy of the CASI imagery. Classes were selected to provide exhaustive coverage of all the relevant features and land uses in the study area. The survey was conducted in March 2003. The study area was known to the lead author and no change in land use occurred in the area in the period between image acquisition and the survey. The winter acquisition of both imagery and field survey meant that the vegetation was dormant in both cases and deciduous trees were not in leaf.

4. Results

4.1. CASI 1 m

4.1.1. Visual interpretation

Table 2 shows the results of the visual interpretation of the imagery. Most of the features of interest can be identified visually on the 1 m resolution CASI imagery. Exceptions are features that are characterised by height differences: flood embankment, water depth and bank profile. Outfalls can usually be identified either directly or indirectly, through identification of the plume of the discharge. However, a plume can only be identified if the composition and/or temperature of the released substance are significantly different from that of the receiving water body and if little or no immediate mixing occurs. Some of the features of interest can be submerged during high tide.

4.1.2. Unsupervised classification

Unsupervised classification with a pre-selected number of 50 classes was carried out on the full imagery. The results of this, however, were very poor, with significant confusion between mud and road surfaces, grass and concrete surfaces, shadows, trees and grass and several other classes. Unsupervised classification was thus deemed an inappropriate approach to map hydromorphology and hydromorphic alteration in such environments.

4.1.3. Supervised classification

Fig. 2 shows the result of a supervised classification of the CASI imagery, whereby the image was classified into 13 target classes: building, road, railway track, metal pipe, concrete, boulders, mud, tidal water, inland water, marsh, grass, agriculture, and trees. Detailed maps of smaller areas are shown in Figs. 3 and 4. The error matrix in Table 3 indicates how the classes in the classified image relate to 'real world' classes. Table 3 also shows that the overall accuracy of the map is 72%, with the user accuracy values of the individual classes ranging from 9% (railway track) to 97% (mud).

Distinction between the broad groups of water, mud, man-made surfaces and vegetation is generally good, although there is some confusion between road and mud, where real world mud is classified as road. Confusion between the classes within the broader groups is significantly higher. Buildings, road and railway track are frequently misclassified; metal pipes that are present in the imagery are often classified correctly, but there is some commission since other classes are misclassified as metal pipe. Long shadows from trees, buildings and bridges are another cause of misclassification in many cases. There is significant omission and commission between marsh, grass, agriculture and trees, which have user's accuracies between 32% and 79%.

4.2. CASI 4 m and 10 m

4.2.1. Visual interpretation

Table 2 indicates how a reduction of spatial resolution to 4 and 10 m influences the number of features of interest that can be identified. Many larger features, buildings, bridges, jetties etc., can still be identified particularly on the 4 m imagery, but the smaller features, such as a pipeline or boulders cannot be detected anymore. Tracks and unsealed roads and a number of other important features are generally impossible to detect at 10 m resolution.

Table 2
Results of the visual interpretation of the CASI imagery at different spatial resolutions and LiDAR

Features			1 m resolution Visible?	4 m resolution Visible?	10 m resolution Visible?	LiDAR Visible?
Man-made	Building	Industrial	Yes	Yes	Yes	Yes
		Private	Yes	Yes	Yes	Yes
	Roads, tracks	Sealed road	Yes	Yes	Yes	?
		Unsealed road	Yes	Yes	No	?
		Track	Yes	Yes	No	No
		Bridge	Yes	Yes	Yes	Yes
	Flood defence	Dam	Not present	Not present	Not present	Not present
		Weir	Not present	Not present	Not present	Not present
		Rip-rap	Yes	Yes	Yes	
		Embankment	No	No	No	Yes
		Groyne	Yes	Yes	Yes	Yes
	Other	Jetty	Yes	Yes	Yes	Yes
		Outfall	?	Yes	Yes	?
		Pipe bridge	Yes	Yes	Yes	Yes
Natural	Channel	Width	Yes	Yes	Yes	Yes
		Depth				
		Sinuosity	Yes	Yes	Yes	Yes
		Bank profile	No	No	No	No
		Gravel bar	Not present	Not present	Not present	Not present
		Backwater	Yes	Yes	Yes	Yes
		Boulders	Yes	Yes	Yes	
		Bedrock	Not present	Not present	Not present	Not present
	Land use	Broadleaf woodland	Yes	Yes	Yes	?
		Coniferous woodland	Yes	Yes	Yes	?
		Wetland	Yes	Yes	Yes	?
		Mudflat	Yes	Yes	Yes	?
		Scrub	Yes	Yes	Yes	Yes
		Grass	Yes	Yes	Yes	Yes
		Cereals	Yes	Yes	Yes	Yes

A question mark indicates that only some of the larger of the features were identifiable.

4.2.2. Supervised classification

Supervised classification was carried out only on the 4 m resolution imagery given the visual interpretation showed it to be inadequate for purpose. Fig. 5 shows a detailed view of the classified image. The error matrix and the accuracy assessment are given in Table 4. The classification is very similar to that of the 1 m resolution CASI imagery, although the overall accuracy of 74% is slightly higher than that of the 1 m resolution CASI imagery (72%).

4.3. LiDAR

Some man-made features such as buildings, bridges and flood embankment are readily identified because of their sudden change in height. Similarly, trees can be identified. With respect to rivers, platform, channel form, bank profile and along stream profile can be measured. In addition LiDAR can provide information on historic channel shape and location as this is often reflected in the topography. On the other hand, land-cover types are difficult to classify.

The roughness of the surface can be determined by calculating the standard deviation across a window of x pixels. The roughness image shows all features with sudden height differences, in particular buildings and bridges, but also flood embankments and trees. The surface roughness image added as an extra layer to multi-spectral imagery can improve the classification accuracy. The resultant image is shown in Fig. 6. However, this can be done only for relatively small reaches at a time to limit influence of changes in elevation of features with similar relief relating to decreasing altitudes down the long profile. When (classified) multi-spectral imagery is draped over 3-D LiDAR topography, visual interpretation will improve. A disadvantage is, however, the considerable computer power that is needed.

5. Discussion

5.1. Interpretation of the results

5.1.1. Scale and geometry issues

Critical to identification of features is scale (Legleiter et al., 2002). The 1 m resolution of the CASI image proved adequate for identification of most features of

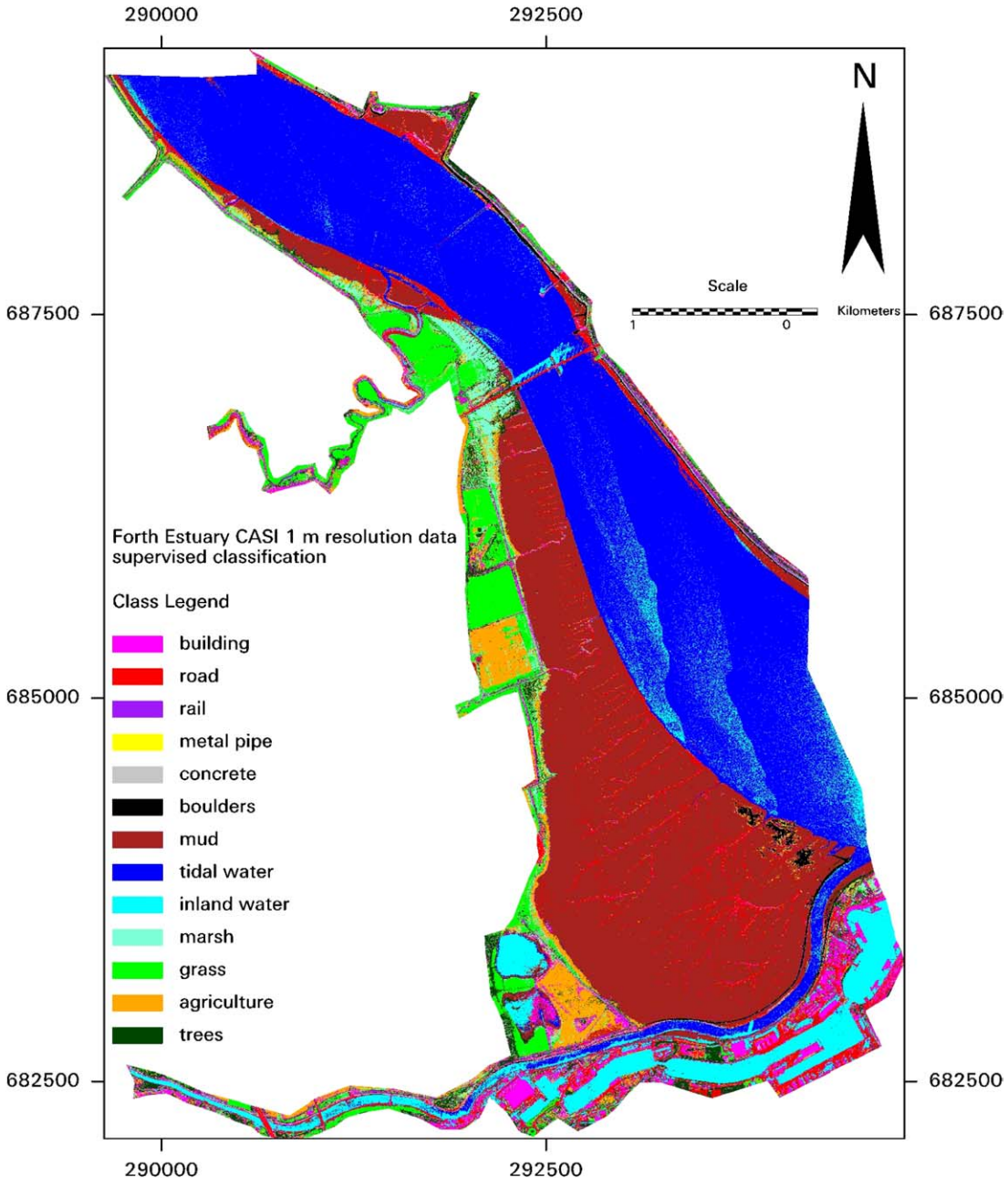

Fig. 2. A supervised classification of the study area using 1 m CASI data.

interest on the estuary and tidal reaches of the River Carron. Given the requirement for vertical imagery, identification of the presence and materials of vertical banks was not possible. These findings support a number of other recent studies of estuarine and riverine mapping using similar spatial resolution imagery (Bryant et al., 1996; Wright et al., 2000; Marcus, 2002; Marcus et al., 2003; Whited et al., 2002; Rainey et al., 2003). The improved classification accuracies achieved with degradation from 1 to 4 m, however, is unusual. The small percentage improvement resulted from the 'smoothing' effect of the pixel degradation, as the smaller variations in pixel value are averaged. For example, some 1 m pixels over water with sun glint or totally in shadow were misclassified but when degraded to 4 m the sun glint or shadow became a smaller component of the overall spectral signature of the pixel and resulted in correct classification. These effects are thought to be a scene-specific function of the spatial variability of land cover types and interferences with their typical spectral signature. Degradation to 4 m is not recommended as a universal procedure. Overall, given the scale of land cover types, the 1 m spatial resolution was best for purpose and only led to a few errors. At the land–water

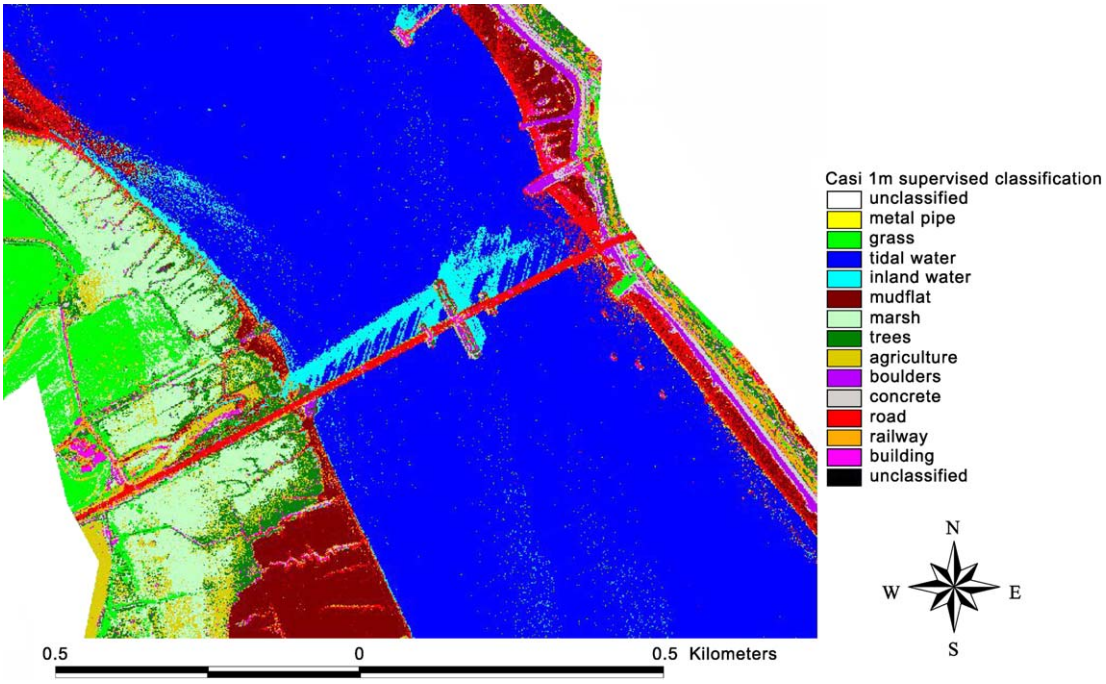

Fig. 3. A zoom-in of the Kincardine bridge study reach using 1 m CASI data. The location is shown in Fig. 1.

interface, for example, mixed pixels occasionally led to misclassification. Degradation of the imagery to 4 m, resulted in smaller features (e.g. pipes) not being identifiable. Degradation to 10 m although allowing the gross morphology to be depicted and major alteration features to be recognised (e.g. urban/industrial areas/road bridges) resulted in smaller features of interest not being visible. Imagery with lower spatial resolution than 4 m results in a rapid loss of useful information; with 4 m pixels, features have to be greater than 12 m in diameter/width if most of their pixels are not going to be a mix of land cover types. Beyond the estuary shoreline the scale of land cover types and features were generally less than this and led to the 10 m imagery being deemed not fit for purpose. Overall, the inaccuracies observed were due mainly to the fact that in the scene there are gradual transitions between some land cover types (e.g. saltmarsh and mudflats). Low classification accuracies in the vicinity of ecotonal environments thus emerge that are solely the inadequacies of boundary representation imposed by field surveyors. The authors agree with Legleiter (2003) who argues that the imagery is better at mapping the intrinsic spatial complexity of river and similar type aquatic systems and results in improved portrayal of gradational zones between adjacent features. Indeed,

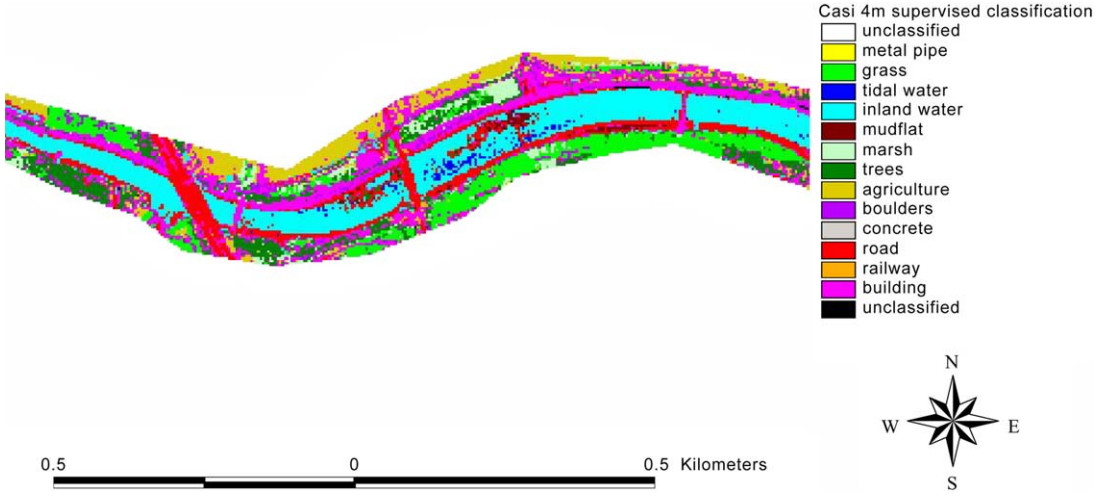

Fig. 4. A zoom-in of a reach of the River Carron using 1 m CASI data. The location is shown in Fig. 1.

Table 3
Error matrix and accuracy assessment for the supervised classification of the Forth estuary CASI 1 m resolution data. The top row shows the 'correct' (based on ground truthing and visual interpretation of the photographs) reference classes. The first column shows the classes on the classified image. The diagonal numbers (shaded) indicate how many pixels were correctly classified by the unsupervised classification method. The remaining numbers show to what 'incorrect' classes the misclassified pixels were allocated

	Reference data															
Classified data and unsupervised classification	**Buildings**	**Tarmac roads**	**Railway track**	**Metal outfalls**	**Concrete**	**Boulders (rip-rap)**	**Mudflat**	**Saline water**	**Freshwater**	**Saltmarsh**	**Grass**	**Cereals**	**Woodland**	**Row total**	**Producer's accuracy (%)**	**User's accuracy (%)**
Building	14	1		1	11		2				3	6	2	40	42.42	35.00
Tarmac roads	6	14					20	4	3			3		50	46.67	28.00
Railway track	5	4	3			1	8			6	3	1	2	33	60.00	9.09
Metal outfalls	1	2	1	3	1	1		1	2					12	75.00	25.00
Concrete	4	2			16	1	3			2		3	1	32	45.71	50.00
Boulders (rip-rap)		1			2	16	8	1		1		1		30	84.21	53.33
Mudflat							163		3			2		168	78.37	97.02
Saline water								211	6				1	218	90.95	96.79
Freshwater		3					1	13	54					71	79.41	76.06
Saltmarsh										26	6	3		35	44.07	74.29
Grass	1						3	1		13	7	24		49	48.00	48.98
Cereals					2					3	42	6		53	62.69	79.29
Woodland	2	3	1		3			1		8	6	1	12	37	66.67	32.43
Column total	33	30	5	4	35	19	208	232	68	59	67	50	18	828		
Overall classification accuracy = 72.22%																

this was demonstrated by the fact that Legleiter et al. (2002) improved river habitat classification accuracies by 15.5% by removal of transitional areas using interior buffers. This improvement in classification accuracy was far beyond that obtained by them using enhanced spatial resolution; using 1 m as opposed to 2.5 m pixel data gave an increased performance of only 4.7%.

5.1.2. Spectral discrimination

Where visible, the estuarine morphology form of inflowing rivers and the presence of man-made features can usually be visually identified by their form and spectral properties. Automated classification using spectral properties however can be difficult where only subtle differences exist between the spectral properties of different features. For example, man-made features may not be differentiated from natural features because they are made of natural materials, are partially colonised by lichens and higher plants, the feature geometry and pixel size of them lead to mixed pixels with natural land cover types and/or shadow alter their reflectance. Shadow and sun glint appear to be universal problems (Wright et al., 2000; Marcus, 2002; Whited et al., 2002). In addition, there is the problem of the absence of discrete spectral signatures and hence classification in ecotonal environments as discussed above under scale and geometry issues. These complications in this study led to automated classification procedures having accuracy values of not greater than 74% for the whole scene; although individual features sometimes could be identified more accurately. However, given that shadow was extensive due to winter acquisition and the northerly latitude of the location and the fact that there was no correction for limb brightening, the results may be a worst case scenario (in the absence of clouds). The extensive shadow cast was most likely the primary cause of the poor unsupervised accuracy values along the River Carron where trees and buildings were in close proximity to the river bank and waters edge. Given the problem of shadow new image analysis techniques are being tested that involves a combination of (1) simulation of areas of shading using the topographic information generated from LiDAR and a knowledge of sun zenith and azimuth at the time of imagery capture and (2) separate classification of shaded areas (Spowage et al., submitted for publication). Also flood embankments covered in tarmac or grass although obvious on the ground due to their topographic form and in imagery due to their linear pattern, cannot be spectrally differentiated. LiDAR offers possibilities in combination

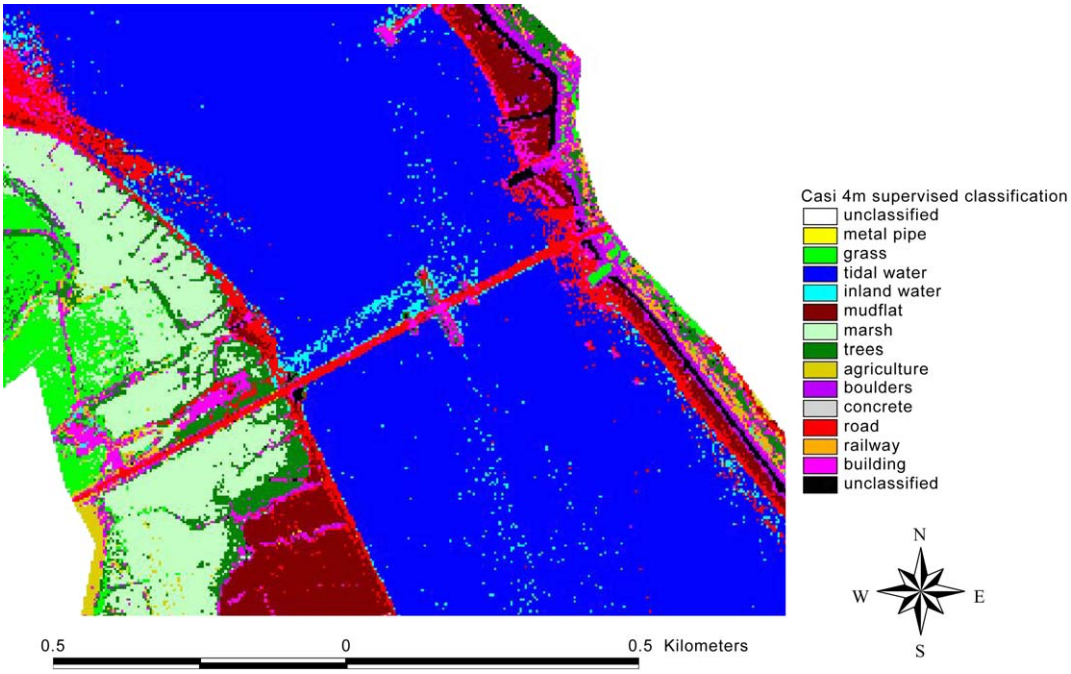

Fig. 5. A zoom-in of the Kincardine bridge study reach using 4 m CASI data (area as in Fig. 3).

with spectrally based classification because it adds topographic information (Hugg and Wehr, 1997) that may differentiate the feature from surrounding areas. The turbid waters of estuaries usually results in there being limited opportunities for bathymetric mapping using hyper-spectral imagery in contrast to such undertaking in clearer waters of upstream reaches and coastal waters (Gilvear et al., 1995; Winterbottom and Gilvear, 1997). Certain types of LiDAR, however, offer the possibility of mapping bathymetry (e.g. Irish and Lillycrop, 1999; Guenther et al., 2000). The infrared (1064 nm) and blue–green (532 nm) regions of the spectrum give best water penetration and water–air interface detection. The SHOALS LiDAR system described by Irish and Lillycrop (1999) has such water penetrating capability. Since laser energy is reduced through reflection, scattering and absorption at the water surface, in the water itself and on the bottom, optical water clarity and bottom type are the main limiting factors for depth detection. As a general rule, LiDAR bathymeters can collect depth information up to 3 times the Secchi disc depth. Accuracy for the SHOALS system is 1–3 m in the horizontal direction and 15 cm for vertical heights/depths.

5.2. Assessment of the feasibility of using colour aerial photography and multi-spectral imagery to map hydromorphology and hydromorphic alteration

This study was undertaken in the context of an investigation into the feasibility of using remotely sensed data to monitor hydromorphology and hydromorphic alteration on estuaries, rivers and lakes so that member states can comply with the WFD. The study has demonstrated the possibility of gaining panoptic coverage using either visual or automated methodologies if nation-wide high spatial resolution multi-spectral imagery is available. With regard to the specific requirements of the WFD to monitor hydromophological elements imagery can provide information regarding river continuity, morphological conditions and water width, structure and substrate of the bed above the water line and structure of the riparian zone. A wide variety of potential difficulties may be apparent however in comprehensively mapping all elements, particularly using automated classification. Difficulties include features being obscured by overhead tree canopies, coverage of artificial features by natural vegetation preventing their easy visual detection, the need for clear water to measure depth and submerged substrates, sun glint on water surfaces and shadow confusing automated classification procedures. Thus this study only gained overall classification accuracy value of between 72% and 74%; these levels of accuracy hiding higher and lower values for particular features of interest. Such levels of detection accuracy have been reported elsewhere in the literature in similar type studies and using similar imagery (Wright et al., 2000; Whited et al., 2002; Marcus, 2002). Observation of the below water-line hydromorphology and submerged features is problematic using hyper-spectral imagery in the turbid waters of the lower reaches of rivers and estuaries but as stated above is possible using some types of LiDAR. Imagery

Table 4
Error matrix and accuracy assessment for the supervised classification of the Forth estuary CASI 4 m resolution data. The top row shows the 'correct' (based on ground truthing and visual interpretation of the photographs) reference classes. The first column shows the classes on the classified image. The diagonal numbers (shaded) indicate how many pixels were correctly classified by the unsupervised classification method. The remaining numbers show to what 'incorrect' classes the misclassified pixels were allocated

	Reference data															
Classified data and unsupervised classification	**Buildings**	**Tarmac roads**	**Railway track**	**Metal outfalls**	**Concrete**	**Boulders (rip-rap)**	**Mudflat**	**Saline water**	**Freshwater**	**Saltmarsh**	**Grass**	**Cereals**	**Woodland**	**Row total**	**Producer's accuracy (%)**	**User's accuracy (%)**
Buildings	28	7	1	1	22	1	7	2	8	5	7	7	3	99	84.85	28.28
Tarmac roads	3	15		1			20	7	2			1		49	50.00	30.61
Railway track		1	2										1	4	40.00	50.00
Metal outfalls														0	*	*
Concrete		1	1	2	5	3	2			1	2		1	18	14.29	27.78
Boulders (rip-rap)						13	6	1						20	68.42	65.00
Mudflat						1	171		1	2				175	82.21	97.71
Saline water							1	211	6				1	219	90.95	96.35
Freshwater	1	2			1		1	11	51					67	75.00	76.12
Saltmarsh		1			1					35	3	4		44	59.32	79.55
Grass	1				3	1				2	40	6	1	54	59.07	74.07
Cereals										4	3	28	1	36	56.00	77.77
Woodland		3	1		3					10	12	4	10	43	55.55	23.26
Column total	33	30	5	4	35	19	208	232	68	59	67	50	18	828		

Overall classification accuracy = 73.55%

acquisition under low water level conditions is recommended to minimise the areas of substrate hidden even with such LiDAR. The requirements of the WFD to monitor the hydromorphological elements of hydrological regime, quantity and dynamics of water flows and connection to groundwater bodies are unlikely to be solved solely using imagery in the near future.

Two questions arise out of this work. Firstly "does remotely sensed data provide a pragmatic and rigorous approach to mapping estuarine and tidal river hydromorphology and hydromorphic alteration". Secondly if the answer to the first question is yes "does mapping have to be undertaken by manual interpretation or can automated classification be used to facilitate, enhance and quicken the process"? In relation to the first question the answer appears to be yes. Spaceborne sensors such as IKONOS and QUICKBIRD, although lacking hyperspectral capability now have the spatial resolution (<4 m) to identify the morphology of channels in the order of 30 m or more in width. At such a scale and the water extent across most of channel at least 5 unmixed pixels will be present. Obviously however if the channel has a complex morphology with mid-channel sand banks bars as in a braided system or emergent vegetation the higher spatial resolution capability of airborne imagery may be required. The advantages of spaceborne data are coverage and cost per unit area but apart from the problem of spectral and spatial resolution, cloud cover can also be a problem in moist temperate climates. As an example from 335 Landsat TM images covering parts of Scotland between November 2001 and November 2002 only 3.5% showed a cloud cover of less than 30%; the summer of 2002 in Scotland was even more cloudy than normal! In winter months the problem of shadow removal or classification with shaded areas also requires tackling by sophisticated image analysis techniques. The timing of the satellite overpasses has changed significantly however from, for example, a 16-day repeat cycle for Landsat and similar for IRS and SPOT imagery, to a 3-day repeat cycle for the new generation satellites such as IKONOS and QUICKBIRD improving the likelihood for cloudless skies. The new generation satellites also have the advantage of a programmable viewing geometry and can acquire imagery up to 700 km sideways, which

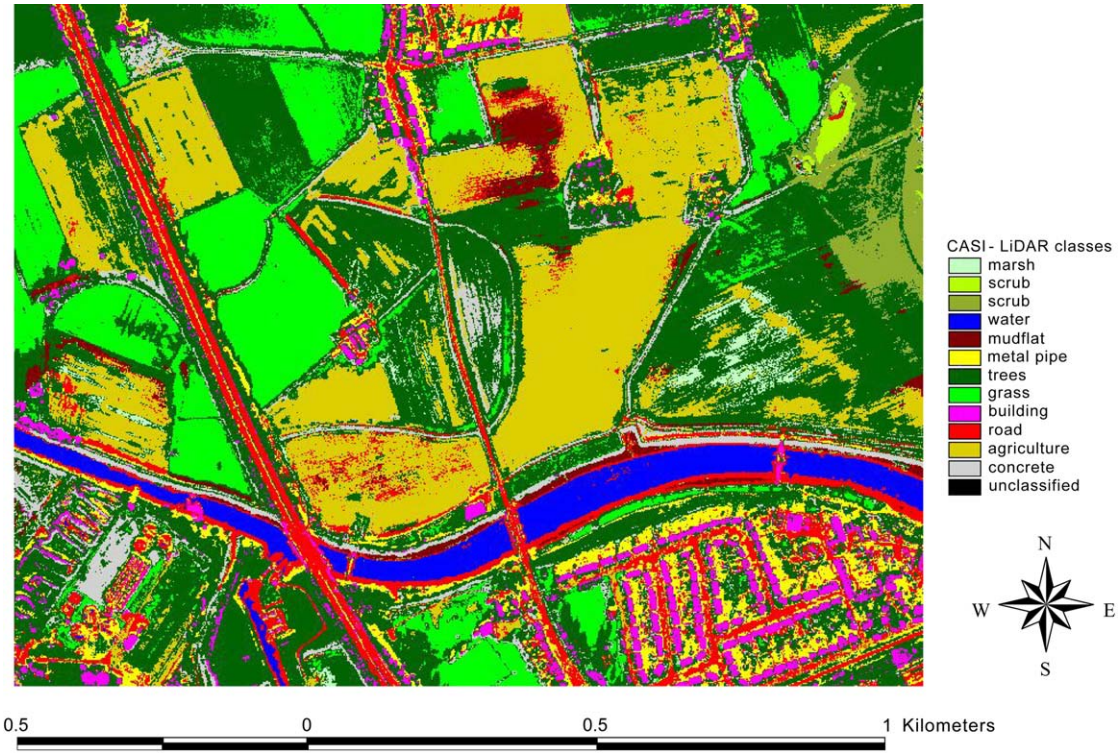

Fig. 6. A classification of the River Carron and floodplain using 1 m CASI data and LiDAR combined (area as in Fig. 4).

means that the same area can be covered on different overpasses.

Tidal waters smaller than 20 m width will require imagery obtained from airborne platforms. Multi-spectral data can be flown at sub 1 m scale and aerial photography with ground resolutions of less than 0.5 m is becoming widely available. Aerial photography is likely to have panoptic coverage but multi and hyper-spectral imagery may often not be available and will need to be commissioned for a particular estuary. The flexibility of being able to fly under ideal atmospheric conditions and at noon to minimise shadows brings added benefits. Aerial photography is also likely to be relatively cheap with costs of under £20 per km.

With regard to the second question "does mapping have to be undertaken by manual interpretation or can automated classification be used to facilitate, enhance and quicken the process?", it is given that visual assessment techniques provide the most reliable approach to identifying features on the imagery. However, automated classification procedures have quite good accuracy and provide rapid assessments with the number of features, and aerial coverage of features all compiled automatically and geo-referenced. There is also considerable scope for a classification accuracy above that achieved in this and other studies (Wright et al., 2000; Whited et al., 2002; Marcus, 2002; Legleiter et al., 2002) all of which have deployed relatively simple classification procedures. New developments include adding topographic information, as determined for example from LiDAR as an additional layer in the classification. Use of artificial intelligence techniques, that can take into account shape attributes may also prove fruitful in this context. Such expert systems are based on symbolic representation and incorporate qualitative data into the estimation through prior programming of the learning algorithm.

6. Conclusion

Airborne multi-spectral imagery and LiDAR proved to be a useful tool for mapping and monitoring the hydromorphology and human modifications of the Forth estuary and tidal reaches of the approximately 30 m wide River Carron. The results showed that features of interest were visible on the high spatial imagery (1 m). On smaller systems higher spatial resolution imagery may be required and increasingly with channel narrowing shadow becomes a greater problem, particularly where tall buildings lie adjacent to the water body because they dominate scenes and the water–land boundary which is of particular interest. This was apparent on the visual assessment of the CASI imagery for the Leith area of Edinburgh where four storey buildings dominate the sky line and cast long shadows across the waterfront and into the estuary. On the Forth estuary and tidal waters of the River Carron automated classification accuracy was

between 72 and 74%, although individual feature recognition varied. The classification procedures, however were relatively simple and more intelligent systems may be able to yield higher values.

With continuing improvements in imagery and an increasing research effort into improved means of automated classification methods, remotely sensed assessments of estuaries and tidal waters at the national scale could become a reality. In the context of the strict requirements of the WFD for monitoring at the national scale this could become important for member states. From a research perspective it will also allow synoptic studies of the way estuaries and tidal rivers respond to sea level rise, land claim, and coastal realignment.

Acknowledgements

This study was undertaken as part of a Scottish Environmental Protection Agency contract (Ref No 230/4144) titled "A feasibility study to assess the usefulness of remote sensing data to assess surface and groundwaters". We also acknowledge the imagery of the estuary provided by the Scottish Executive. Useful comments by Dr W. Andrew Marcus at the review stage also helped to improve the paper.

References

Batholdy, J., Folving, S., 1986. Sediment classification and surface type mapping in the Danish Wadden Sea by remote sensing. Netherlands Journal of Sea Research 20, 337–345.

Bryant, R.G., Tyler, A., Gilvear, D.J., McDonald, P., Teasdale, I., Ferrier, G., 1996. A preliminary investigation into the VNIR spectral characteristics of inter-tidal estuarine sediments. International Journal of Remote Sensing 19, 405–412.

Bryant, R.G., Gilvear, D.J., 1999. Quantifying geomorphic and riparian land cover changes either side of a large flood event using airborne remote sensing: River Tay, Scotland. Geomorphology 29, 307–321.

Cobby, D.M., Mason, D.C., Davenport, I.J., 2001. Image processing of airborne laser altimetry data for improved river flood modelling. Journal of Photogrammetry and Remote Sensing 56, 121–138.

Charlton, M.E., Large, A.R.G., Fuller, I.C., 2003. Application of airborne LiDAR in river environments: the River Coquet, Northumberland, UK. Earth Surface Processes and Landforms 28, 299–306.

Donoghue, D.N., Reid Thomas, D.C., Zong, Y., 1994. Mapping and monitoring the intertidal zone of the east coast using remote sensing techniques and a coastal monitoring GIS. Marine Technology Society 28, 19–29.

Gilvear, D.J., Waters, T.M., Milner, A.M., 1995. Image analysis of aerial photography to quantify changes in channel morphology and instream habitat following placer mining in interior Alaska. Freshwater Biology 34, 389–398.

Gilvear, D.J., Bryant, R., Hardy, T., 1999. Remote sensing of channel morphology and instream fluvial processes. Progress in Environmental Science 1, 257–284.

Gilvear, D.J., Bryant, R., 2003. Aerial photography and other remotely sensed data. In: Kondolf, M., Piegey, H. (Eds.), Tools in Fluvial Geomorphology. John Wiley and Sons, Chichester, pp. 211–247.

Gilvear D.J., Davids, C., Tyler, A. Evaluation of the feasibility of using remotely sensed data to detect hydromorphology and hydromophic alteration; River Tummel, Scotland. River Research and Applications, in press.

Guenther, G.C., Brooks, M.W., LaRocque, P.E., 2000. New capabilities of the "SHOALS" airborne LiDAR bathymeter. Remote Sensing of Environment 73, 247–255.

Hardy, T.B., Anderson, P.C., Neal, C.M.U., Stevens, D.K., 1994. Application of multispectral videography for the deliniation of riverine depths and mesoscale hydraulic features. Paper and presentation at the American Water Resources Association, Effects on Human Induced Changes on Hydrologic Systems, June 26–29, 1994. Jackson Hole, Wyoming.

Horritt, M.S., Mason, D.C., Cobby, D.M., Davenport, D.I., Bates, P.D., 2003. Waterline mapping in flooded vegetation from airborne SAR imagery. Remote Sensing of Environment 85, 271–281.

Hugg, C., Wehr, A., 1997. Detecting and identifying topographic objects in imaging laser altimetry data. International Archives of Photogrammetry and Remote Sensing 32 (Part 3–4W2), 19–26.

Irish, J.L., Lillycrop, W.J., 1999. Scanning laser mapping of the coastal zone: the SHOALS system. Journal of Photogrammetry and Remote Sensing 54, 123–129.

Legleiter, C., Marcus, W.A., Lawrence, R., 2002. Effects of sensor resolution on mapping instream habitats. Photogrammetric Engineering and Remote Sensing 68, 801–807.

Legleiter, C.J., 2003. Spectrally driven classification of high spatial resolution, hyperspectral imagery: a tool for mapping instream habitat. Environmental Management 32, 399–411.

Leuven, R.S.E., Pudevigne, I., Teuww, R.M., 2002. Application of Geographical Information Systems and Remote Sensing in River Studies. Backhuys publishers, Leiden, The Netherlands, 246 pp.

Marcus, W.A., 2002. Mapping of instream microhabitats with high spatial resolution hyperspectral imagery. Journal of Geographical Systems 4, 113–126.

Marcus, W.A., Legleiter, C.J., Aspinall, Boardman, J., Crabtree, R., 2003. High spatial resolution, hyperspectral (HSRH) mapping of instream habitats, depths, and woody debris in mountain streams. Geomorphology 55, 363–380.

McClusky, D.S., 1987. Intertidal habitats and benthic macrofauna of the Forth estuary, Scotland. Proceedings of the Royal Society of Edinburgh 93B, 389–399.

McManus, J., Duck, R.W., Anderson, J.M., 1999. The relative merits and limitations of thermal radiometric measurements in estuarine studies. International Journal of Remote Sensing 20, 549–559.

Milton, E.J., Gilvear, D.J., Hooper, I.D., 1995. Investigating change in fluvial systems using remotely sensed data. In: Gurnell, A., Petts, G. (Eds.), Changing River Channels. John Wiley and Sons, Chichester, pp. 276–301.

Muller, E., Decamps, H., Dobson, M.K., 1993. Contribution of space remote sensing to river studies. Freshwater Biology 29, 301–312.

Rainey, M.P., Tyler, A.N., Gilvear, D.J., Bryant, R.G., McDonald, P., 2003. Mapping intertidal estuarine sediment grain size distributions through airborne remote sensing. Remote Sensing of Environment 86, 480–490.

Spowage, G., Gilvear, D.J., Tyler, A., Winterbottom, S.J. Automated classification of river and floodplain habitat using remotely sensed data; tackling the shadow problem. International Journal of Remote Sensing, submitted for publication.

Thomson, A.G., Fuller, R.M., Sparks, T.H., Yates, M.G., Eastwood, J.A., 1998. Ground and airborne radiometry over inter-tidal surfaces: waveband selection for cover classification. International Journal of Remote Sensing 19, 1189–1205.

van der Wal, D., Pye, K., Neal, A., 2002. Long-term morphological change in the Ribble estuary, north west England. Marine Geology 189, 249–266.

Webb, A.J., Metcalfe, A.P., 1987. Physical aspects, water movements and modelling studies of the Forth estuary, Scotland. Proceedings of the Royal Society of Edinburgh 93B, 259–272.

Westaway, R.M., Lane, S.N., Hicks, D.M., 2000. The development of an automated correction procedure for digital photogrammetry for the study of wide, shallow, gravel-bed rivers. Earth Surface Processes and Landforms 25, 209–226.

Winterbottom, S.J., Gilvear, D.J., 1997. Quantification of channel bed morphology in gravel-bed rivers using airborne multispectral imagery and aerial photography. Regulated Rivers: Research and Management 13, 489–499.

Whited, D., Stanford, J.A., Kimball, J.S., 2002. Application of airborne multispectral imagery to quantify riverine habitats at different base flows. River Research and Applications 18, 583–594.

Witte, C.R., Dowling, D. Weller, R. Denham, R., Rowland, T., 2001. Quantifying riparian vegetation and stream bank form through the use of airborne laser scanning and digital video data. Proceedings of International Geoscience and Remote Sensing Symposium, 9–13 July 2001, Sydney, Australia, pp. 1545–1548.

Wright, A., Marcus, W.A., Aspinall, R., 2000. Evaluation of multispectral, fine scale digital imagery as a tool for mapping stream morphology. Geomorphology 33, 107–120.

Yates, M.G., Jones, A.R., McGrorty, S., Goss-custard, J.D., 1993. The use of satellite imagery to determine the distribution of inter-tidal surface sediments of the Wash, England. Estuarine, Coastal and Shelf Science 36, 333–334.